



# ***Exact Solution for Electro- Thermo- Mechanical Behavior of Composite Cylinder Reinforced by BNNTs under Non- Axisymmetric Thermo- Mechanical Loads***

A. Ghorbanpour Arani<sup>1\*</sup>, E. Haghparast<sup>2</sup>, Z. Khoddami Maraghi<sup>3</sup>, S. Amir<sup>4</sup>

1- Professor, Faculty of Mechanical Engineering, University of Kashan, Kashan, Iran

2- Ph.D Student Department of Mechanical Engineering, University of Kashan, Kashan, Iran

3- Ph.D Student Department of Mechanical Engineering, University of Kashan, Kashan, Iran

4- Assistant Potfessor, Department of Mechanical Engineering, University of Kashan, Kashan, Iran

## **ABSTRACT**

In this research, static stresses analysis of boron nitride nano - tube reinforced composite (BNNTRC) cylinder made of poly - vinylidene fluoride (PVDF) subjected to non - axisymmetric thermo - mechanical loads and applied voltage is developed. The surrounded elastic medium is modelled by Pasternak foundation. Composite structure is modeled based on piezoelectric fiber reinforced composite (PFRC) theory and a representative volume element has been considered for predicting the elastic, piezoelectric and dielectric properties of the cylinder. Higher order governing equations were solved analytically by Fourier series. The results demonstrated that the fatigue life of BNNTRC cylinder will be significantly dependent on the angle orientation and volume fraction of BNNTs. Results of this investigation can be used for the optimum design of thick - walled cylinders under the multi - physical fields.

## **KEYWORDS**

Composite Hollow Cylinder, Non - Axisymmetric Temperature Distribution, PFRC Theory, Pasternak Foundation, BNNTs Fibers.

---

\*Corresponding Author, Email: aghorban@kashanu.ac.ir

## 1- INTRODUCTION

BNNTs have the same atomic structure as carbon nanotubes (CNTs) but there exist many interesting properties including a more stable electronic property and better resistance to oxidation at high temperatures. BNNTs potential applications consist of different mechanically - reinforced materials such as polymer, ceramic, and metal composites, and key parts of nano - electro - mechanical smart systems.

In this decade, analytical thermo - mechanical stress calculations for thick - walled cylinder have been investigated. Dai et al. [1] presented electro - magneto - thermo - elastic behavior of a hollow cylinder composed of functionally graded piezoelectric material (FGPM), placed in a uniform magnetic field, subjected to electric, thermal and mechanical loads. They showed that applying suitable electric, thermal and mechanical loads could optimize the FGPM hollow cylindrical structures. In this regard, Poultangari et al. [2] studied an analytical method to obtain the solution for the two - dimensional steady state thermal and mechanical stresses in a hollow thick sphere made of functionally graded material (FGM). Their results indicated that the radial, tangential, and shear stress distributions can be reduced in magnitude when the power law index assumes the smaller values. Electro - thermo - elastic stress analysis of piezoelectric polymeric thick - walled cylinder, reinforced by BNNTs subjected to electro - thermo - mechanical fields, is presented by Ghorbanpour Arani et al. [3] who showed that increasing DWBNNTs content reduces the stresses associated with mechanical, thermal and electrical fields, in descending order. Similarly, Ghorbanpour Arani et al. [4] studied thermal stress analysis of a thick - walled cylinder reinforced with FG single - walled carbon nanotubes (SWCNTs). The higher order governing equation was solved in order to obtain the distribution of displacement and thermal stresses in radial, circumferential and longitudinal directions. FG distributions of SWCNTs have significant effect on displacements and thermal stresses of composite cylinder, so that in incrementally increasing layout, the radial and circumferential stresses are lower than the other FG structures.

Recently, Jafari Fesharaki et al. [5] developed the

general theoretical analysis of a FG piezoelectric hollow cylinder subjected to the two - dimensional electro - mechanical load. They used separation of variables method and complex Fourier series, to derive and solve the Navier equations in terms of displacements. Their study revealed, using this method and considering the special boundary conditions and material properties for a hollow cylinder, the mechanical and electrical displacements and stresses can be controlled and optimized. The analytical solution of FG piezoelectric hollow cylinder, which is under the radial electric potential and non - axisymmetric thermo - mechanical loads, are presented by Atrian et al. [6] who used complex Fourier series to indicate the distributions of stresses, displacement and the effect of electric potential field on the cylinder behavior.

However, to date, no report has been found in the literature on the stress analysis of composite cylinder reinforced by BNNTs under non - axisymmetric thermo - mechanical loads. Motivated by these considerations, the need for the investigation of a BNNTs fiber is applied as reinforcement in composite cylinder where PVDF has been selected for matrix as piezoelectric material. Composite cylinder is subjected to non - axisymmetric thermo - mechanical loads and applied voltage. Higher order governing equations are derived analytically and effects of non - axisymmetric pressure, volume fraction and orientation angle of BNNTs on the stresses are investigated. Results of this research could be used for the optimum design of composite cylinder under non - axisymmetric thermo - mechanical loadings.

## 2- GOVERNING EQUATIONS

### A. Heat solution

Fig. 1, ” illustrates a thick-walled cylinder subject to the temperature distribution  $T(r, \theta)$  which is reinforced by BNNT fiber in radial direction. Temperature distribution has been applied in a hollow cylinder under a non-axisymmetric heat conduction caused by non-axisymmetric thermal boundary conditions. This is like to having a cylinder exposed to a given heat flux on a part of its outer boundary while on the other part a specified temperature is applied. The general distribution of temperature ( $T(r, \theta)$ ) in hollow cylinder with inside and

outside radii  $a$  and  $b$ , respectively, can be written as [7]:

where  $A_0$  and  $B_0$  are the arbitrary constants and the functions  $F_0(r)$  and  $G_n(r)$  can be determined for different boundary conditions. The first term at the right - hand side of Eq. (1),  $A_0$ , produces a uniform axial stress for a thick cylinder in the plane strain condition. The second term causes such stresses being as a function of the radius and the terms under the summation signs produce non - axisymmetric thermal stresses. All terms automatically satisfy Michell condition and they don't contribute to the thermal stresses, except for the terms associated with  $n = 0$  and  $n = 1$ . Therefore, Eq. (1) can be simplified to:

$$T(r, \theta) = F_0(r) + F_1(r) \cos \theta + G_1(r) \sin \theta. \quad (2)$$

where the functions  $F_0(r)$ ,  $F_1(r)$  and  $G_1(r)$  are determined by boundary conditions. Using stress boundary condition in inner and outer radius, non - axisymmetric temperature distribution can be expressed as follows:

$$T(r, \theta) = \frac{A_0}{r} \cos \theta + \frac{B_0}{r} \sin \theta. \quad (3)$$

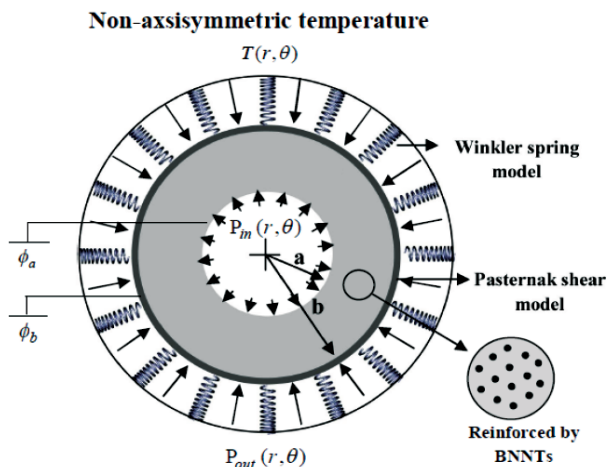


Figure 1: The schematic of composite cylinder under non - axisymmetric temperature and pressure distribution and applied voltage.

In axisymmetric heat conduction,  $T(r) = T_d \ln(r/a) + T_a$ , ( $T_d = T_a - T_b$ ) introduces the symmetric temperature distribution in which  $T_a$  and  $T_b$  are the inside and outside temperatures of the cylinder, respectively. Therefore, the general solution for heat conduction can be expressed as [7]:

$$T(r, \theta) = T_{\text{non-axisymmetric}} + T_{\text{axisymmetric}} \\ = \frac{A_0}{r} \cos \theta + \frac{B_0}{r} \sin \theta + T_d \ln \frac{r}{a} + T_a. \quad (4)$$

«Figs. 2 - a and 2 - b, » show the distribution of temperature in radial and circumferential directions where the temperature distribution is the combination of axisymmetric and non - axisymmetric temperature terms. «Fig. 2 - b,» depicts temperature distribution in particular angle where the curves have logarithmic distribution based on Eq. (4).

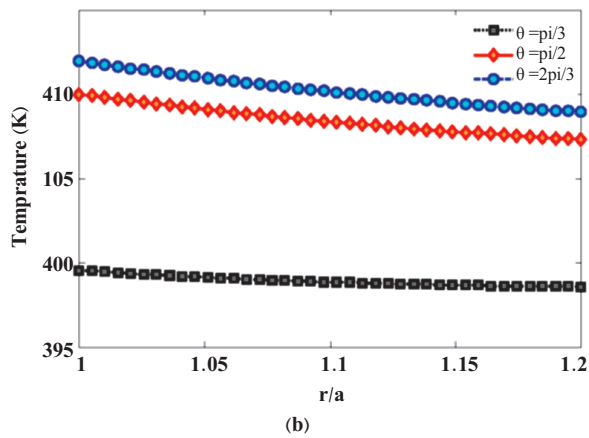
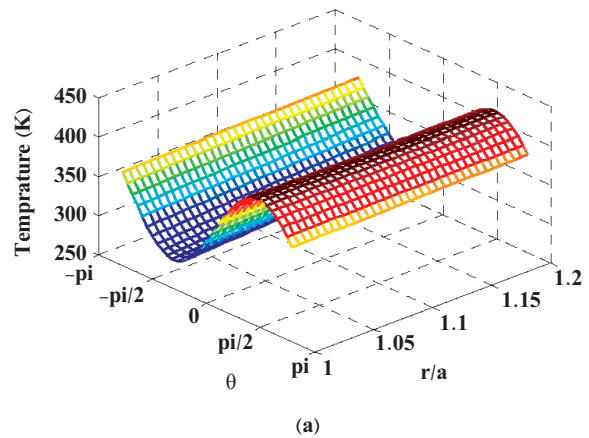


Figure 2: Non - axisymmetric temperature distribution.

## B. Stress analysis

Composite cylinder reinforced by BNNTs under non - axisymmetric loadings embedded in an elastic medium has been demonstrated in “Fig.1”. The strain - displacement relations in cylindrical coordinate can be written as [5]:

$$\epsilon_{rr} = \frac{\partial u}{\partial r}, \quad (5 - a)$$

$$\epsilon_{\theta\theta} = \frac{1}{r} \left( \frac{\partial v}{\partial \theta} \right) + \frac{u}{r}, \quad (5 - b)$$

$$\varepsilon_{r\theta} = \frac{1}{2} \left( \frac{1}{r} \left( \frac{\partial u}{\partial \theta} \right) + \frac{\partial v}{\partial r} - \frac{v}{r} \right) \quad (5 - c)$$

where u and v are the components of displacement in radial and circumferential, respectively.

### c. Micro - electro - mechanical model

To model the smart composite structures, a micromechanical model known as “XY PEFRC” or “YX PEFRC”, using an approach adopted by Tan and Tong [8, 9], is employed. Based on this modeling, the reinforced BNNTs are considered as longitudinal straight fibers placed in PVDF matrix. In a general case, to evaluate the effective properties of a PFRC unit cell in all directions, first, the properties of the required strip is obtained in which an appropriate ‘X model’ in association with the ‘Y model’ (or vice versa), i.e., ‘XY (or YX) rectangle model’ has been employed. In this modeling, both matrix and reinforcements are assumed to be smart and the polarization has been made along the fiber direction. According to the XY PEFRC micromechanical method, the constitutive equations for the electro - thermo - mechanical behavior of the selected RVE are expressed as [10]:

$$\begin{Bmatrix} \sigma \\ D \end{Bmatrix} = \begin{bmatrix} C & -e \\ e^T & \epsilon \end{bmatrix} \begin{Bmatrix} \varepsilon \\ E \end{Bmatrix} \quad (6)$$

where  $\sigma$ ,  $\varepsilon$ , D and E are stress, strain, electric displacement and electric field vectors, respectively and  $[e]$  and  $[\epsilon]$  are matrices of piezoelectric and dielectric parameters respectively.

Eq. (6) can be expanded as follows:

$$\begin{Bmatrix} \sigma_1 \\ \sigma_2 \\ \sigma_3 \\ \tau_3 \\ \tau_3 \\ \tau_2 \\ D_1 \\ D_2 \\ D_3 \end{Bmatrix} = \begin{bmatrix} C_1 & C_2 & C_3 & 0 & 0 & 0 & 0 & 0 & -e_3 \\ C_2 & C_2 & C_3 & 0 & 0 & 0 & 0 & 0 & -e_3 \\ C_3 & C_3 & C_3 & 0 & 0 & 0 & 0 & 0 & -e_3 \\ 0 & 0 & 0 & C_4 & 0 & 0 & 0 & -e_3 & 0 \\ 0 & 0 & 0 & 0 & C_5 & 0 & -e_5 & 0 & 0 \\ 0 & 0 & 0 & 0 & 0 & C_6 & 0 & 0 & 0 \\ 0 & 0 & 0 & 0 & e_5 & 0 & \epsilon_1 & 0 & 0 \\ 0 & 0 & 0 & e_3 & 0 & 0 & 0 & \epsilon_2 & 0 \\ e_3 & e_3 & e_3 & 0 & 0 & 0 & 0 & 0 & \epsilon_3 \end{bmatrix} \begin{Bmatrix} \varepsilon_1 \\ \varepsilon_2 \\ \varepsilon_3 \\ \gamma_3 \\ \gamma_3 \\ \gamma_2 \\ E_1 \\ E_2 \\ E_3 \end{Bmatrix} \quad (7)$$

Assuming the plane strain condition and unidirectional electric field along the radius of composite cylinder, Eq. (7) is reduced to [10]:

$$\begin{Bmatrix} \sigma_{rr} \\ \sigma_{\theta\theta} \\ \tau_{r\theta} \\ D_r \end{Bmatrix} = [Q] \begin{Bmatrix} \varepsilon_{rr} \\ \varepsilon_{\theta\theta} \\ \gamma_{r\theta} \\ E_r \end{Bmatrix} \quad (8)$$

where matrix  $[Q]$  is defined as [10]:

$$[Q] = \begin{bmatrix} C_{rrrr} & C_{rr\theta\theta} & 0 & -e_{rrr} \\ C_{rr\theta\theta} & C_{\theta\theta\theta\theta} & 0 & -e_{r\theta\theta} \\ 0 & 0 & C_{r\theta r\theta} & 0 \\ e_{rrr} & e_{r\theta\theta} & 0 & \epsilon_r \end{bmatrix} \quad (9)$$

Electric field in the radial direction of cylindrical coordinate for piezoelectric materials is [5]:

$$E_r = -\frac{\partial \phi}{\partial r} \quad (10)$$

where  $\phi$  denotes the scalar function of the electric potential.

To consider the effects of orientation angle of the BNNTs with respect to the longitudinal axis, the following transformation matrix can be employed as [10]:

$$[\tilde{Q}] = [T][Q][T]^T \quad (11)$$

The transformation matrix  $[T]$  is:

$$[T] = \begin{bmatrix} \cos^2 \alpha & \sin^2 \alpha & 2 \sin \alpha \cos \alpha & 0 \\ \sin^2 \alpha & \cos^2 \alpha & 2 \sin \alpha \cos \alpha & 0 \\ -\sin \alpha \cos \alpha & \sin \alpha \cos \alpha & \cos^2 \alpha - \sin^2 \alpha & 0 \\ 0 & 0 & 0 & 1 \end{bmatrix} \quad (12)$$

where  $\alpha$  is the angle of BNNTs with respect to the longitudinal axis of composite cylinder.

### D. Equilibrium equations

The equilibrium equations in the radial and circumferential directions, regarding the body forces are [5]:

$$\frac{\partial \sigma_{rr}}{\partial r} + \frac{1}{r} \frac{\partial \sigma_{r\theta}}{\partial \theta} + \frac{\sigma_{rr} - \sigma_{\theta\theta}}{r} + F_{body\ force} = 0, \quad (13 - a)$$

$$\frac{\partial \sigma_{r\theta}}{\partial r} + \frac{1}{r} \frac{\partial \sigma_{\theta\theta}}{\partial \theta} + \frac{2 \sigma_{r\theta}}{r} = 0, \quad (13 - b)$$

$$\frac{\partial D_r}{\partial r} + \frac{D_r}{r} = 0. \quad (13 - c)$$

Thick - walled cylinder surrounded by elastic medium that is simulated with Pasternak foundation where the effect of the elastic medium has been considered as body force on the outer surface of cylinder as below [10]:

$$\begin{aligned} F_{Pasternak} &= K_w u - G_p \nabla^2 u \\ &= K_w u - G_p \left( \frac{\partial^2 u}{\partial r^2} + \frac{1}{r} \frac{\partial u}{\partial r} + \frac{1}{r^2} \frac{\partial^2 u}{\partial \theta^2} \right). \end{aligned} \quad (14)$$

Substituting Eqs. (14) into Eq. (13) and by using Eqs. (5) and (8), the final equilibrium equations, in terms of displacements and electrical potential, can be

determined as follows:

$$d_1 \frac{\partial^2 u}{\partial r^2} + \frac{d_2}{r} \frac{\partial u}{\partial r} + \frac{d_3}{r^2} u + \frac{d_4}{r^2} \frac{\partial^2 u}{\partial \theta^2} + \frac{d_5}{r} \frac{\partial^2 v}{\partial r \partial \theta} + \frac{d_6}{r^2} \frac{\partial v}{\partial \theta} + d_7 \frac{\partial^2 \phi}{\partial r^2} + \frac{d_8}{r} \frac{\partial \phi}{\partial r} = 0, \quad (15 - a)$$

$$d_9 \frac{\partial^2 v}{\partial r^2} + \frac{d_{10}}{r} \frac{\partial v}{\partial r} + \frac{d_{11}}{r^2} v + \frac{d_{12}}{r^2} \frac{\partial^2 v}{\partial \theta^2} + \frac{d_{13}}{r} \frac{\partial^2 u}{\partial r \partial \theta} + \frac{d_{14}}{r^2} \frac{\partial u}{\partial \theta} + \frac{d_{15}}{r^2} \frac{\partial^2 \phi}{\partial r \partial \theta} = 0, \quad (15 - b)$$

$$d_{16} \frac{\partial^2 \phi}{\partial r^2} + \frac{d_{17}}{r} \frac{\partial \phi}{\partial r} + d_{18} \frac{\partial^2 u}{\partial r^2} + \frac{d_{19}}{r} \frac{\partial u}{\partial r} + \frac{d_{20}}{r} \frac{\partial^2 v}{\partial r \partial \theta} = 0. \quad (15 - c)$$

where the constants  $d_1$  to  $d_{20}$  are given in the appendix A.

### 3- SOLVING METHOD

Eqs. (15 - a) to (15 - c) are governing the equations for a thick - walled composite cylinder under electro - mechanical fields. In general solution of Eqs.15, the radial, circumferential displacements and electric potential are presumed according to the complex Fourier series form [11]:

$$u(r, \theta) = \sum_{n=-\infty}^{\infty} u_n(r) e^{in\theta}, \quad (16 - a)$$

$$v(r, \theta) = \sum_{n=-\infty}^{\infty} v_n(r) e^{in\theta}, \quad (16 - b)$$

$$\phi(r, \theta) = \sum_{n=-\infty}^{\infty} \phi_n(r) e^{in\theta} = \phi_0(r). \quad (16 - c)$$

where  $u_n(r)$  and  $v_n(r)$  are the coefficients of complex Fourier series of  $u(r, \theta)$  and  $v(r, \theta)$ , respectively, that can be expressed as:

$$u_n(r) = \frac{1}{2\pi} \int_{-\pi}^{\pi} u(r, \theta) e^{-in\theta} d\theta, \quad (17 - a)$$

$$v_n(r) = \frac{1}{2\pi} \int_{-\pi}^{\pi} v(r, \theta) e^{-in\theta} d\theta. \quad (17 - b)$$

and electric potential just depends on the radius of composite cylinder. Therefore, Eq. (16 - c) is valid only for  $n = 0$  and it will be omitted for  $n \neq 0$  [6].

For  $n \neq 0$ , substituting Eq. (16) into Eq. (15) gives:

$$d_1 u_n'' + \frac{d_2}{r} u_n' + \left( \frac{d_3}{r^2} - n^2 \frac{d_4}{r^2} \right) u_n + \frac{d_5}{r} v_n' + \frac{d_6}{r^2} v_n = 0, \quad (18 - a)$$

$$d_9 v_n'' + \frac{d_{10}}{r} v_n' + \left( \frac{d_{11}}{r^2} - n^2 \frac{d_{12}}{r^2} \right) v_n + \frac{d_{13}}{r} u_n' + \frac{d_{14}}{r^2} u_n = 0. \quad (18 - b)$$

The solutions of the above equations are assumed as [11]:

$$u_n(r) = Ar^\eta, \quad (19 - a)$$

$$v_n(r) = Br^\eta. \quad (19 - b)$$

where  $A$  and  $B$  are constants and obtained from the boundary conditions. Substituting Eq.(19) into Eqs.(18), yields:

$$\left[ d_1 \eta(\eta - 1) + d_2 \eta + d_3 - n^2 d_4 \right] A + \left[ ind_5 \eta + ind_6 \right] B = 0, \quad (20 - a)$$

$$\left[ d_9 \eta(\eta - 1) + d_{10} \eta + d_{11} - n^2 d_{12} \right] B + \left[ ind_{13} \eta + ind_{14} \right] A = 0. \quad (20 - b)$$

To obtain the nontrivial solution of Eq. (20), the determinant of the system should be equal to zero [5]. So four roots,  $\eta_{n1}$  to  $\eta_{n4}$ , are achieved and the general solutions are:

$$u_n(r) = \sum_{j=1}^4 A_{nj} r^{\eta_{nj}}, \quad (21 - a)$$

$$v_n(r) = \sum_{j=1}^4 M_{nj} A_{nj} r^{\eta_{nj}}. \quad (21 - b)$$

where:

$$M_{nj} = - \frac{d_1 \eta(\eta - 1) + d_2 \eta + d_3 - n^2 d_4}{ind_5 \eta + ind_6}, \quad (22)$$

For  $n=0$ , the equilibrium Eqs. (15) are reduced to:

$$d_1 u_0'' + \frac{d_2}{r} u_0' + \frac{d_3}{r^2} u_0 + d_7 \phi_0'' + \frac{d_8}{r} \phi_0' = 0, \quad (23 - a)$$

$$d_9 v_0'' + \frac{d_{10}}{r} v_0' + \frac{d_{11}}{r^2} v_0 = 0, \quad (23 - b)$$

$$d_{16} \phi_0'' + \frac{d_{17}}{r} \phi_0' + d_{18} u_0'' + \frac{d_{19}}{r} u_0' = 0. \quad (23 - c)$$

where the subscript zero indicates the solution for  $n=0$ . Two equations (23 - a) and (23 - c) are a coupled ordinary differential equations and the solution of these are considered as [11]:

$$u_0(r) = A_0 r^{\eta_0}, \quad \phi_0(r) = C_0 r^{\eta_0}. \quad (24 - a)$$

Substituting Eq. (24 - a) into Eqs. (23 - a) and (23 - c)

yields:

$$(d_1\eta_0(\eta_0 - 1) + d_2\eta_0 + d_3)A_0 + (d_7\eta_0(\eta_0 - 1) + d_8\eta_0)C_0 = 0,$$

$$(d_{16}\eta_0(\eta_0 - 1) + d_{17}\eta_0)C_0 + (d_{18}\eta_0(\eta_0 - 1) + d_{19}\eta_0)A_0 = 0. \quad (24 - b)$$

To obtain the nontrivial solution of Eq. (24 - b), the determinant of the system should be equal to zero. So the four roots,  $\eta_{01}$  to  $\eta_{04}$ , are achieved and the general solutions are:

$$u_0(r) = \sum_{j=1}^4 A_{0j} r^{\eta_{0j}}, \quad \phi_0(r) = \sum_{j=1}^4 N_{0j} A_{0j} r^{\eta_{0j}}. \quad (25 - a)$$

$$N_{0j} = -\frac{d_1\eta_0(\eta_0 - 1) + d_2\eta_0 + d_3}{d_7\eta_0(\eta_0 - 1) + d_8\eta_0}. \quad (25 - b)$$

For  $n = 0$  Eq. (23 - b) is a decoupled ordinary differential equation and the solution of this equation is considered as:

$$v_0(r) = \sum_{j=5}^6 A_{0j} r^{\eta_{0j}}. \quad (26 - a)$$

$$\eta_{05, 06} = \frac{-d_{10} \pm \sqrt{d_{10}^2 - 4d_9d_{11}}}{2d_9}. \quad (26 - b)$$

Finally substituting Eqs. (24 - a), (25 - a) and (26 - a) into Eq. (16), general solutions for  $u(r, \theta)$ ,  $v(r, \theta)$  and  $\phi(r)$  are expressed as:

$$u(r, \theta) = \sum_{j=1}^4 A_{0j} r^{\eta_{0j}} + \sum_{n=-\infty, n \neq 0}^{\infty} \left[ \sum_{j=1}^4 A_{nj} r^{\eta_{nj}} \right] e^{in\theta}, \quad (27 - a)$$

$$v(r, \theta) = \sum_{j=5}^6 A_{0j} r^{\eta_{0j}} + \sum_{n=-\infty, n \neq 0}^{\infty} \left[ \sum_{j=1}^4 M_{nj} A_{nj} r^{\eta_{nj}} \right] e^{in\theta}, \quad (27 - b)$$

$$\phi(r) = \sum_{j=1}^4 N_{0j} A_{0j} r^{\eta_{0j}}. \quad (27 - c)$$

Substituting Eqs. (27 - a) - (27 - c) into Eq. (5), the strains are obtained as:

$$\varepsilon_{rr}^M = \left[ \sum_{j=1}^4 \eta_{0j} A_{0j} r^{(\eta_{0j}-1)} \right]$$

$$+ \sum_{n=-\infty, n \neq 0}^{\infty} \left[ \sum_{j=1}^4 \eta_{nj} A_{nj} r^{(\eta_{nj}-1)} \right] e^{in\theta}, \quad (28 - a)$$

$$\varepsilon_{\theta\theta}^M = \left[ \sum_{j=1}^4 A_{0j} r^{(\eta_{0j}-1)} \right]$$

$$+ \sum_{n=-\infty, n \neq 0}^{\infty} \left[ \sum_{j=1}^4 A_{nj} r^{(\eta_{nj}-1)} \right] e^{in\theta}$$

$$+ n \sum_{n=-\infty, n \neq 0}^{\infty} \left[ \sum_{j=1}^4 M_{nj} A_{nj} r^{(\eta_{nj}-1)} \right] e^{in\theta}, \quad (28 - b)$$

$$\varepsilon_{r\theta}^M = \frac{1}{2} \left\{ in \sum_{n=-\infty, n \neq 0}^{\infty} \left[ \sum_{j=1}^4 A_{nj} r^{(\eta_{nj}-1)} \right] e^{in\theta} \right.$$

$$\left. + \sum_{n=-\infty, n \neq 0}^{\infty} \left[ \sum_{j=1}^4 \eta_{nj} M_{nj} A_{nj} r^{(\eta_{nj}-1)} \right] e^{in\theta} \right.$$

$$\left. - \left[ \sum_{j=5}^6 A_{0j} r^{(\eta_{0j}-1)} \right] \right.$$

$$\left. - \sum_{n=-\infty, n \neq 0}^{\infty} \left[ \sum_{j=1}^4 M_{nj} A_{nj} r^{(\eta_{nj}-1)} \right] e^{in\theta} \right\}. \quad (28 - c)$$

Substituting Eqs. (28 - a) - (28 - c) into Eq. (8) and using Eqs. (9) and (27 - c), the stress components and the electrical displacement in the radial direction are calculated in Appendix B.

For  $n \neq 0$ , equilibrium equations require four boundary conditions to satisfy. Expanding the given boundary conditions in complex Fourier series gives the following equation:

$$g_j(\theta) = \sum_{n=-\infty}^{\infty} G_j(n) e^{in\theta}, \quad j = 1, \dots, 6, \quad (29 - a)$$

where:

$$G_j(n) = \frac{1}{2\pi} \int_{-\pi}^{\pi} g_j(\theta) e^{-in\theta} d\theta, \quad j = 1, \dots, 6. \quad (29 - b)$$

Constants  $A_{nj}$  are calculated using Eqs. (28) and (29).

#### 4- NUMERICAL RESULTS AND DISCUSSION

Consider a thick-walled cylinder with inner radius  $a = 1m$  and outer radius  $b = 1.2m$  [11]. The cylinder is embedded in a Pasternak foundation with  $G_p = 2.071273 N/m$  [12]. In this study, the PVDF and BNNT have been taken into account for smart matrix and fiber of the composite cylinder, respectively. In the part of axisymmetric of temperature distribution, the temperature at the inner and outer surfaces have been assumed to be  $T_a = 350K$  and  $T_b = 300K$ , respectively. The thermal expansion coefficients of the composite cylinder in  $r$ ,  $z$  and  $\theta$

directions can be written as [13]:

$$\alpha_r = (1 + \nu_z^{BNNT}) c_r \alpha_r^{BNNT} + (1 + \nu_m) c_m \alpha^m - \nu_\xi \times \alpha_z, \quad (30-a)$$

$$\alpha_z = c_r \alpha_z^{BNNT} + c_m \alpha^m, \quad (30-a)$$

$$\alpha_r = \alpha_\theta, \quad (30-a)$$

$$\nu_\xi = c_r \nu_z^{BNNT} + c_m \nu_m. \quad (30-a)$$

where  $\alpha_z^{BNNT}$  and  $\alpha_r^{BNNT}$  are thermal expansion coefficients of BNNTs in longitudinal and radial directions, respectively, and  $\alpha^m$  is the thermal expansion coefficient of PVDF and assumed to be  $\alpha^m = 7.1 \times 10^{-5} (K)$  [14]. However,  $\alpha_z^{BNNT}$  and  $\alpha_r^{BNNT}$  are not expected to vary significantly for the temperature range of  $200K < T < 400K$  considered in this work. Hence, their average values are taken at  $300K$ . Therefore, they are assumed to be  $\alpha_z^{BNNT} = 1.2 \times 10^{-6}/K$  and  $\alpha_r^{BNNT} = 0.6 \times 10^{-6}/K$

[12].  $\nu_r^{BNNT}$  and  $\nu_m$  are Poisson's ratios of BNNTs and matrix and are taken as  $\nu_z^{BNNT} = 0.34$  and  $\nu_m^{BNNT} = 0.39$  [12].

As mentioned in the previous sections, in order to achieve the total stresses, the thermal and mechanical stresses are calculated separately and finally superposed. The complete solution for stresses, due to the temperature distribution (Eq. (4)), is obtained through the superposition of the axisymmetric and non - axisymmetric stresses. Hence, these stresses are calculated as [7]:

$$\sigma_{rr} = \frac{E\alpha T_d}{2(1-\nu)} \left[ -\ln \frac{r}{a} + \frac{b^2}{b^2-a^2} \left(1 - \frac{a^2}{r^2}\right) \ln \frac{b}{a} \right] + \frac{E\alpha r}{2(1-\nu)(a^2+b^2)} \left(1 - \frac{a^2}{r^2}\right) \left(1 - \frac{b^2}{r^2}\right) (A_0 \cos \theta + B_0 \sin \theta), \quad (31-a)$$

$$\sigma_{\theta\theta} = \frac{E\alpha T_d}{2(1-\nu)} \left[ -1 - \ln \frac{r}{a} + \frac{b^2}{b^2-a^2} \left(1 + \frac{a^2}{r^2}\right) \ln \frac{b}{a} \right] + \frac{E\alpha r}{2(1-\nu)(a^2+b^2)} \left(3 - \frac{a^2+b^2}{r^2} - \frac{a^2 b^2}{r^4}\right) (A_0 \cos \theta + B_0 \sin \theta), \quad (31-b)$$

$$\sigma_{r\theta} = \frac{E\alpha r}{2(1-\nu)(a^2+b^2)} \left(1 - \frac{a^2}{r^2}\right) \left(1 - \frac{b^2}{r^2}\right) (A_0 \sin \theta - B_0 \cos \theta) \quad (31-c).$$

Therefore, the thermal stresses in radial and circumferential directions are shown in «Figs. 3 and 4,» and thermal shear stress is depicted in «Fig. 5,» based on Eqs. 31. These figures confirm the harmonic pattern presented in the above equations.

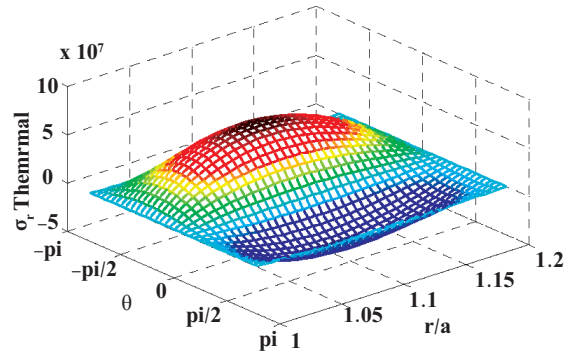


Figure 3: Radial thermal stress in composite cylinder under non - axisymmetric loadings.

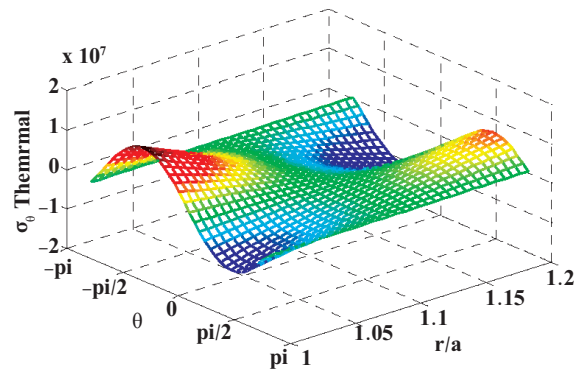


Figure 4: Circumferential thermal stress in composite cylinder under non - axisymmetric loadings.

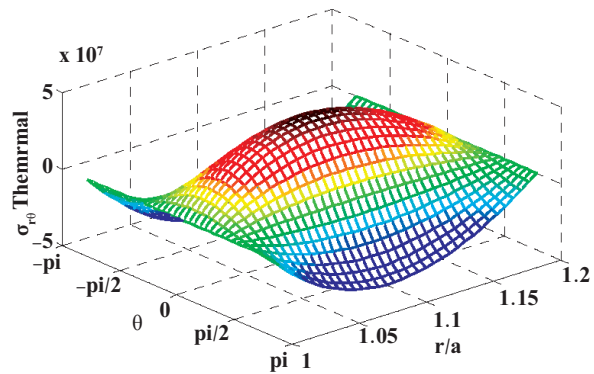


Figure 5: Shear thermal stress in composite cylinder under non - axisymmetric loading.

In order to examine the proposed solution, the effect of two - dimensional thermo - mechanical behavior of piezoelectric composite cylinder is considered. The inside and outside cylinder and the boundary conditions are expressed as [6]:

$$\begin{aligned} S_{rr}(r=a) &= 400 \cos^2 \theta \text{ Mpa}, \\ S_r(r=b) &= 300 \cos^2 \theta \text{ Mpa}, \\ S_{r\theta}(r=a) &= 0, \quad S_{r\theta}(r=b) = 0, \\ \phi(r=a) &= 0, \quad \phi(r=b) = 300. \end{aligned} \quad (32)$$

«Figs. 6 - 8,» demonstrate the distribution of radial, circumferential and shear total stresses. It is evident that all components of stresses and electric displacement follow from a harmonic pattern. Likewise, it can be seen from «Fig. 8,» that the shear total stress is zero at the inner and outer surfaces due to the assumed boundary conditions.

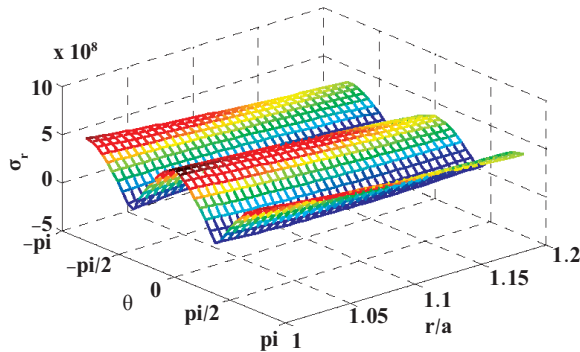


Figure 6: Radial total stress in composite cylinder under electro - thermo - mechanical loadings.

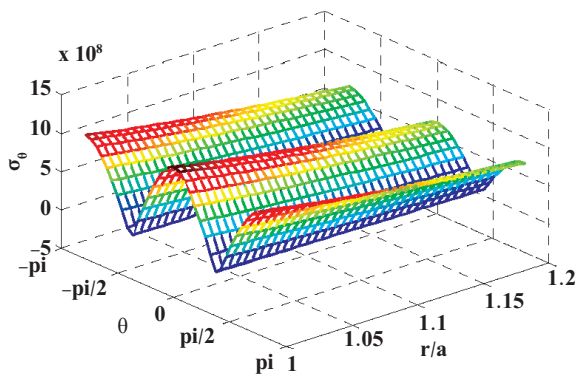


Figure 7: Circumferential total stress in composite cylinder under electro - thermo - mechanical loadings.

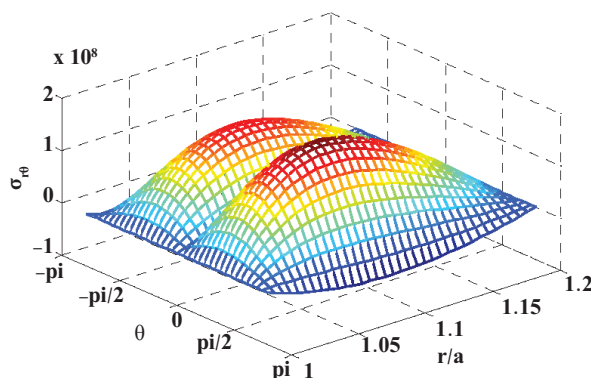


Figure 8: Shear total stress in composite cylinder under electro - thermo - mechanical loadings.

Effective stress as Von - Mises stress has been illustrated in «Fig. 9, » .As expected; the effective stress follows from a harmonic pattern.

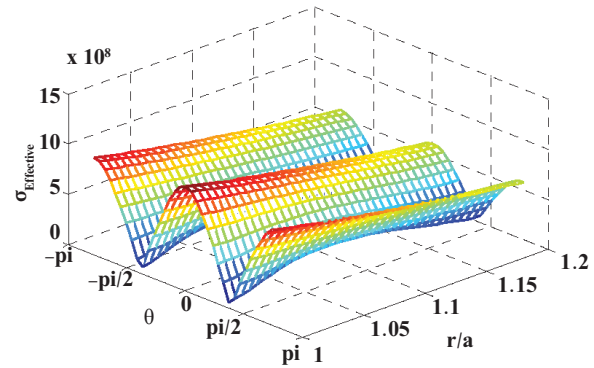


Figure 9: The effective stress in composite cylinder under electro - thermo - mechanical loadings.

«Fig. 10,» shows electric displacement distribution along the radius and circumferential directions. It is also noted that the patterns of «Figs. 6 - 10,» are consistent with reference [5].

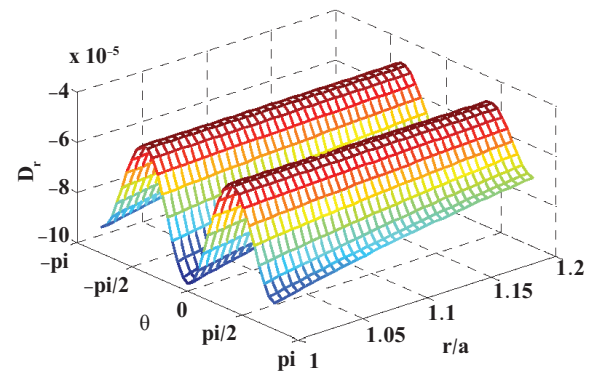


Figure 10: Radial electric displacement in composite hollow cylinder.

According to general boundary conditions (Eq. 32), the inside and outside boundary conditions have been simplified to study the effect of volume fraction, elastic medium and Lorentz force on Von - Mises stress in composite cylinder, as follows:

$$\begin{aligned}
 S_{rr}(r=a) &= -50 \text{ Mpa}, S_{rr}(r=b) = -100 \text{ Mpa}, \\
 S_{r\theta}(r=a) &= 0, S_{r\theta}(r=b) = 0, \\
 \phi(r=a) &= 0, \phi(r=b) = 300.
 \end{aligned}
 \tag{33}$$

Thermal stresses for  $\theta=\pi$  are added to mechanical stresses.

«Fig. 11,» shows the effect of volume fraction on Von - Mises stress in composite cylinder. It can be seen from this figure that increasing volume content of BNNTs causes to decrease Von - Mises stress and leads to increase the strength of composite cylinder. Von - Mises stress is also reduced when the aspect ratio increases.

Designers could meet their purposes by selecting the suitable percent of fiber in composite cylinder.

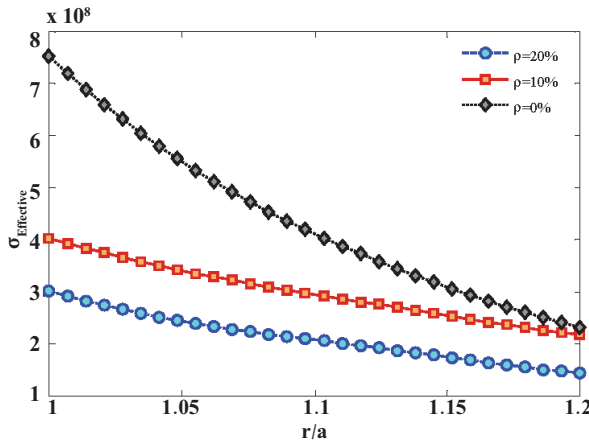


Figure 11: The effect of volume fraction of BNNTs on effective stress in composite cylinder.

The effect of elastic medium on effective stress in composite cylinder is investigated in “Fig. 12,” where the presence of elastic medium has been considered as a factor for increasing the stability of composite cylinder. Here, the Pasternak foundation has been selected due to considering the shear force. As can be seen, increasing Pasternak modulus decreases the effective stress.

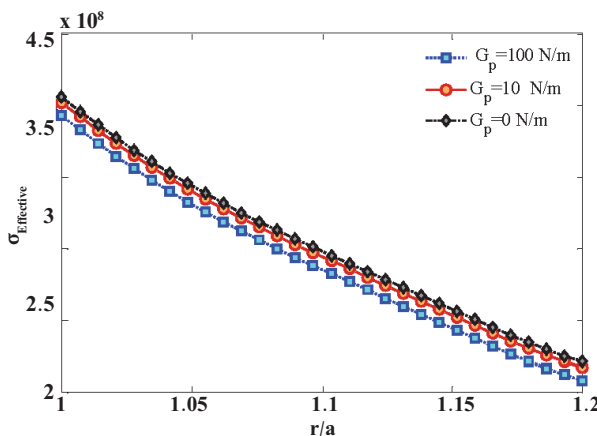


Figure 12: The effect of elastic medium on effective stress in composite cylinder.

“Fig. 13,” illustrates the effect of orientation angle of BNNTs on effective stress in the composite cylinder. The orientation angle of fiber in composite is very important because it can be affected the mechanical behavior of composite. This composite has been reinforced by BNNTs that can be aligned in different direction. Since the purpose is stress analyzing, the angle is the best at which stress is reduced and subsequently displacement slake. It can be concluded that due to the significant radial piezoelectricity effect of BNNT, the

strength of composite cylinder is reduced with decreasing angle of BNNTs with respect to the longitudinal axis.

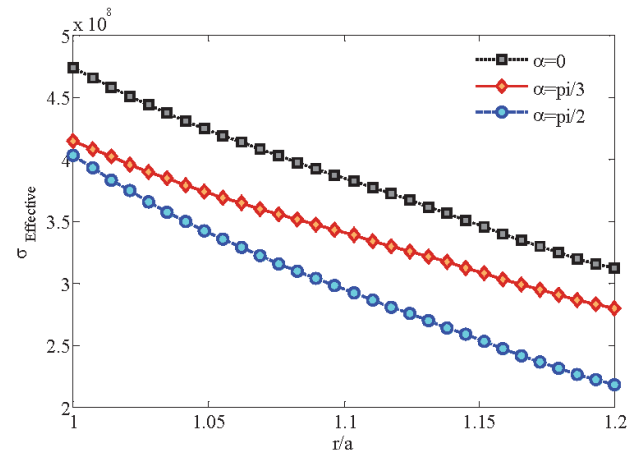


Figure 13: The effect of orientation angle of BNNTs on radial displacement in composite cylinder.

## 5- CONCLUSIONS

Analytical solution , for two - dimensional static stresses for BNNTRC cylinder , was developed under multi - physical fields, where BNNTs are arranged in a longitudinal direction inside of PVDF matrix. The composite cylinder is embedded in an elastic medium as Pasternak foundation which is considering the shear effect. Higher order governing equations were solved analytically by Fourier series and the results illustrate the distribution of thermo - mechanical stresses. 3D figures show a harmonic pattern in stress distribution in spite of non - axisymmetric thermo - mechanical loads that feature the behavior of composite cylinder in different  $r$  and  $\theta$ . It can be observed that using BNNTs as a fiber and its orientation angle with respect to the composite cylinder axis have significant effects on the mechanical behavior of the BNNTRC cylinder. Similarly , it has been found that the magnitude of the effective stress was strongly dependent on the volume fraction of BNNT so that increasing the volume content of BNNTs significantly leads to increase the strength of composite cylinder.

## 6- ACKNOWLEDGEMENT

The authors are grateful to University of Kashan for supporting this work by Grant No. 65475/65. They would like also to thank the Iranian Nanotechnology Development Committee for their financial support.”

## Appendix A

$$[\mathcal{Q}] = [T][\tilde{\mathcal{Q}}][T]^T = \begin{bmatrix} \mathcal{Q}_{11} & \mathcal{Q}_{12} & \mathcal{Q}_{13} & \mathcal{Q}_{14} \\ \mathcal{Q}_{21} & \mathcal{Q}_{22} & \mathcal{Q}_{23} & \mathcal{Q}_{24} \\ \mathcal{Q}_{31} & \mathcal{Q}_{32} & \mathcal{Q}_{33} & \mathcal{Q}_{34} \\ \mathcal{Q}_{41} & \mathcal{Q}_{42} & \mathcal{Q}_{43} & \mathcal{Q}_{44} \end{bmatrix}$$

$$\begin{aligned} d_1 &= \mathcal{Q}_{11} - G_P, & d_2 &= \mathcal{Q}_{12} + \mathcal{Q}_{11} - \mathcal{Q}_{21} - G_P, \\ d_5 &= \mathcal{Q}_{12} + \mathcal{Q}_{33}, & d_6 &= -(\mathcal{Q}_{33} + \mathcal{Q}_{22}), \\ d_9 &= d_{10} = -d_{11} = \mathcal{Q}_{33}, & d_{13} &= \mathcal{Q}_{21} + \mathcal{Q}_{33}, \\ d_{16} &= d_{17} = -\mathcal{Q}_{44}, & d_{18} &= \mathcal{Q}_{41}, \\ d_3 &= -d_{12} = -\mathcal{Q}_{22} - K_w, & d_7 &= -\mathcal{Q}_{14}, \\ d_{14} &= \mathcal{Q}_{22} + \mathcal{Q}_{33}, & d_{19} &= \mathcal{Q}_{41} + \mathcal{Q}_{42}, \\ d_4 &= \mathcal{Q}_{33} - G_P, & d_8 &= -(\mathcal{Q}_{14} - \mathcal{Q}_{24}), \\ d_{15} &= -\mathcal{Q}_{24}, & d_{20} &= \mathcal{Q}_{42} \end{aligned}$$

## Appendix B

$$\begin{aligned} \sigma_{rr} &= \tilde{\mathcal{Q}}_{11} \left\{ \sum_{j=1}^6 A_{0j} r^{(\eta_{0j}-1)} + \sum_{n=-\infty, n \neq 0}^{\infty} \left[ \sum_{j=1}^4 A_{nj} r^{(\eta_{nj}-1)} \right] e^{in\theta} \right. \\ &+ in \sum_{n=-\infty, n \neq 0}^{\infty} \left[ \sum_{j=1}^4 M_{nj} A_{nj} r^{(\eta_{nj}-1)} \right] e^{in\theta} \left. \right\} \\ &+ \tilde{\mathcal{Q}}_{12} \left\{ \sum_{j=1}^6 \eta_{0j} A_{0j} r^{(\eta_{0j}-1)} + \sum_{n=-\infty, n \neq 0}^{\infty} \left[ \sum_{j=1}^4 \eta_{nj} A_{nj} r^{(\eta_{nj}-1)} \right] e^{in\theta} \right\} \\ &+ \tilde{\mathcal{Q}}_{13} \left\{ in \sum_{n=-\infty, n \neq 0}^{\infty} \left[ \sum_{j=1}^4 A_{nj} r^{(\eta_{nj}-1)} \right] e^{in\theta} + \sum_{j=1}^6 \eta_{0j} N_{0j} A_{0j} r^{(\eta_{0j}-1)} \right. \\ &+ \sum_{n=-\infty, n \neq 0}^{\infty} \left[ \sum_{j=1}^4 \eta_{nj} M_{nj} A_{nj} r^{(\eta_{nj}-1)} \right] e^{in\theta} - \sum_{j=1}^6 N_{0j} A_{0j} r^{(\eta_{0j}-1)} \\ &- \sum_{n=-\infty, n \neq 0}^{\infty} \left[ \sum_{j=1}^4 M_{nj} A_{nj} r^{(\eta_{nj}-1)} \right] e^{in\theta} \left. \right\} \\ &+ \tilde{\mathcal{Q}}_{14} \left\{ - \sum_{j=1}^6 N'_{0j} \eta_{0j} A_{0j} r^{\eta_{0j}-1} \right\}, \end{aligned}$$

$$\begin{aligned} \sigma_{\theta\theta} &= \tilde{\mathcal{Q}}_{21} \left\{ \sum_{j=1}^6 A_{0j} r^{(\eta_{0j}-1)} + \sum_{n=-\infty, n \neq 0}^{\infty} \left[ \sum_{j=1}^4 A_{nj} r^{(\eta_{nj}-1)} \right] e^{in\theta} \right. \\ &+ in \sum_{n=-\infty, n \neq 0}^{\infty} \left[ \sum_{j=1}^4 M_{nj} A_{nj} r^{(\eta_{nj}-1)} \right] e^{in\theta} \left. \right\} \\ &+ \tilde{\mathcal{Q}}_{22} \left\{ \sum_{j=1}^6 \eta_{0j} A_{0j} r^{(\eta_{0j}-1)} + \sum_{n=-\infty, n \neq 0}^{\infty} \left[ \sum_{j=1}^4 \eta_{nj} A_{nj} r^{(\eta_{nj}-1)} \right] e^{in\theta} \right\} \\ &+ \tilde{\mathcal{Q}}_{23} \left\{ in \sum_{n=-\infty, n \neq 0}^{\infty} \left[ \sum_{j=1}^4 A_{nj} r^{(\eta_{nj}-1)} \right] e^{in\theta} + \sum_{j=1}^6 \eta_{0j} N_{0j} A_{0j} r^{(\eta_{0j}-1)} \right. \\ &+ \sum_{n=-\infty, n \neq 0}^{\infty} \left[ \sum_{j=1}^4 \eta_{nj} M_{nj} A_{nj} r^{(\eta_{nj}-1)} \right] e^{in\theta} - \sum_{j=1}^6 N_{0j} A_{0j} r^{(\eta_{0j}-1)} \\ &- \sum_{n=-\infty, n \neq 0}^{\infty} \left[ \sum_{j=1}^4 M_{nj} A_{nj} r^{(\eta_{nj}-1)} \right] e^{in\theta} \left. \right\} \\ &+ \tilde{\mathcal{Q}}_{24} \left\{ - \sum_{j=1}^6 N'_{0j} \eta_{0j} A_{0j} r^{\eta_{0j}-1} \right\}, \end{aligned}$$

$$\begin{aligned} \sigma_{r\theta} &= \tilde{\mathcal{Q}}_{31} \left\{ \sum_{j=1}^6 A_{0j} r^{(\eta_{0j}-1)} + \sum_{n=-\infty, n \neq 0}^{\infty} \left[ \sum_{j=1}^4 A_{nj} r^{(\eta_{nj}-1)} \right] e^{in\theta} \right. \\ &+ in \sum_{n=-\infty, n \neq 0}^{\infty} \left[ \sum_{j=1}^4 M_{nj} A_{nj} r^{(\eta_{nj}-1)} \right] e^{in\theta} \left. \right\} \\ &+ \tilde{\mathcal{Q}}_{32} \left\{ \sum_{j=1}^6 \eta_{0j} A_{0j} r^{(\eta_{0j}-1)} + \sum_{n=-\infty, n \neq 0}^{\infty} \left[ \sum_{j=1}^4 \eta_{nj} A_{nj} r^{(\eta_{nj}-1)} \right] e^{in\theta} \right\} \\ &+ \tilde{\mathcal{Q}}_{33} \left\{ in \sum_{n=-\infty, n \neq 0}^{\infty} \left[ \sum_{j=1}^4 A_{nj} r^{(\eta_{nj}-1)} \right] e^{in\theta} + \sum_{j=1}^6 \eta_{0j} N_{0j} A_{0j} r^{(\eta_{0j}-1)} \right. \\ &+ \sum_{n=-\infty, n \neq 0}^{\infty} \left[ \sum_{j=1}^4 \eta_{nj} M_{nj} A_{nj} r^{(\eta_{nj}-1)} \right] e^{in\theta} - \sum_{j=1}^6 N_{0j} A_{0j} r^{(\eta_{0j}-1)} \\ &- \sum_{n=-\infty, n \neq 0}^{\infty} \left[ \sum_{j=1}^4 M_{nj} A_{nj} r^{(\eta_{nj}-1)} \right] e^{in\theta} \left. \right\} \\ &+ \tilde{\mathcal{Q}}_{34} \left\{ - \sum_{j=1}^6 N'_{0j} \eta_{0j} A_{0j} r^{\eta_{0j}-1} \right\}, \end{aligned}$$

$$\begin{aligned} D_r &= \tilde{\mathcal{Q}}_{41} \left\{ \sum_{j=1}^6 A_{0j} r^{(\eta_{0j}-1)} + \sum_{n=-\infty, n \neq 0}^{\infty} \left[ \sum_{j=1}^4 A_{nj} r^{(\eta_{nj}-1)} \right] e^{in\theta} \right. \\ &+ in \sum_{n=-\infty, n \neq 0}^{\infty} \left[ \sum_{j=1}^4 M_{nj} A_{nj} r^{(\eta_{nj}-1)} \right] e^{in\theta} \left. \right\} \\ &+ \tilde{\mathcal{Q}}_{42} \left\{ \sum_{j=1}^6 \eta_{0j} A_{0j} r^{(\eta_{0j}-1)} + \sum_{n=-\infty, n \neq 0}^{\infty} \left[ \sum_{j=1}^4 \eta_{nj} A_{nj} r^{(\eta_{nj}-1)} \right] e^{in\theta} \right\} \\ &+ \tilde{\mathcal{Q}}_{43} \left\{ in \sum_{n=-\infty, n \neq 0}^{\infty} \left[ \sum_{j=1}^4 A_{nj} r^{(\eta_{nj}-1)} \right] e^{in\theta} + \sum_{j=1}^6 \eta_{0j} N_{0j} A_{0j} r^{(\eta_{0j}-1)} \right. \\ &+ \sum_{n=-\infty, n \neq 0}^{\infty} \left[ \sum_{j=1}^4 \eta_{nj} M_{nj} A_{nj} r^{(\eta_{nj}-1)} \right] e^{in\theta} - \sum_{j=1}^6 N_{0j} A_{0j} r^{(\eta_{0j}-1)} \\ &- \sum_{n=-\infty, n \neq 0}^{\infty} \left[ \sum_{j=1}^4 M_{nj} A_{nj} r^{(\eta_{nj}-1)} \right] e^{in\theta} \left. \right\} \\ &+ \tilde{\mathcal{Q}}_{44} \left\{ - \sum_{j=1}^6 N'_{0j} \eta_{0j} A_{0j} r^{\eta_{0j}-1} \right\}, \end{aligned}$$

## 7- REFERENCES

- [1] H.L. Dai, L. Hong, Y.M. Fu and X. Xiao, "Analytical solution for electro - magneto - thermo - elastic behaviors of a functionally graded piezoelectric hollow cylinder", Applied Mathematical Modelling, vol. 34, pp. 343 - 357, February, 2010.
- [2] R. Poultangari, M. Jabbari and M.R. Eslami, "Functionally graded hollow spheres under non - axisymmetric thermo - mechanical loads", International Journal of Pressure Vessels and Piping, vol. 85, pp. 295 - 305, May, 2008.
- [3] A. Ghorbanpour Arani, A. Haghshen, S. Amir, M. Azami and Z. Khoddami Maraghi, "Electro - Thermo - Mechanical Response of Thick - Walled Piezoelectric Cylinder Reinforced by BNNTs", Journal of Nanostructures, vol. 2, pp.

- 113 - 124, April, 2012.
- [4] A. Ghorbanpour Arani, S. Amir, V. Sadooghi and M. Mohammadimehr, "Thermal Stress Analysis of a Composite Cylinder Reinforced with FG SWCNTs", *Journal of Solid Mechanics*, vol. 3, pp. 132 - 141, April, 2011.
- [5] J. Jafari Fesharaki, V. Jafari Fesharaki, M. Yazdipoor and B. Razavian, "Two - dimensional solution for electro - mechanical behavior of functionally graded piezoelectric hollow cylinder", *Applied Mathematical Modelling*, vol. 36, pp. 5521 - 5533, November, 2012.
- [6] A. Atrian, J. Jafari Fesharaki, G.H. Majzoobi and M. Sheidaee, "Effects of Electric Potential on Thermo - Mechanical Behavior of Functionally Graded Piezoelectric Hollow Cylinder under Non - Axisymmetric Loads", *World Academy of Science, Engineering and Technology*, vol. 59, pp. 964 - 967, April, 2011.
- [7] R.B. Hetnarski and M.R.Eslami, "Thermal Stresses - Advanced Theory and Applications", vol. I. New York: Springer, 2009.
- [8] P. Tan and L. Tong, "Micro - electro - mechanics models for piezoelectric - fiber - reinforced composite materials", *Composite Science Technology*, vol. 61, pp. 759 - 769, April, 2001.
- [9] P. Tan and L. Tong, "Micromechanics models for nonlinear behavior of piezoelectric fiber reinforced composite materials", *International Journal of Solids and Structures*, vol. 38, pp. 8999 - 9032, December, 2001.
- [10] A. Ghorbanpour Arani, A.R. Shajari, S. Amir and A. Loghman, "Electro - thermo - mechanical nonlinear nonlocal vibration and instability of embedded micro - tube reinforced by BNNT conveying fluid", *Physica E*, vol. 44, pp. 424 - 432, August, 2012.
- [11] M. Jabbari, S. Sohrabpour and M.R. Eslami, "General Solution for Mechanical and Thermal Stresses in a Functionally Graded Hollow Cylinder due to Non - axisymmetric Steady - State Loads", *Journal of Applied Mechanics*, vol. 70, pp. 111 - 118, January. 2003.
- [12] Z. Khodami Maraghi, A. Ghorbanpour Arani, R. Kolahchi, S. Amir and M.R. Bagheri, "Nonlocal vibration and instability of embedded DWBNNT conveying viscose fluid", *Composites: Part B*, vol. 45, pp. 423 - 432, February, 2013.
- [13] A. Ghorbanpour Arani, M.R. Mozdianfard, V. Sadooghi, M. Mohammadimehr and R. Kolahchi, "Magneto - thermo - elastic Behavior of Cylinder Reinforced with FG SWCNTs under Transient Thermal Field", *Journal of Solid Mechanics*, vol. 3, pp. 1 - 10, February, 2011.
- [14] JE. Mark, *Polymer Data Hand Book*, vol. I. New York: Oxford University Press, 1999.